Cigarette Smoke Induces Cellular Senescence

Toru Nyunoya, Martha M. Monick, Aloysius Klingelhutz, Timur O. Yarovinsky, Jeffrey R. Cagley, and Gary W. Hunninghake

Division of Pulmonary, Critical Care, and Occupational Medicine, and the Department of Microbiology, University of Iowa Roy J. and Lucille A. Carver College of Medicine; and Veterans Administration Medical Center, Iowa City, Iowa

Chronic obstructive pulmonary disease (COPD) is the fourth leading cause of death in the United States, and cigarette smoking is the major risk factor for COPD. Fibroblasts play an important role in repair and lung homeostasis. Recent studies have demonstrated a reduced growth rate for lung fibroblasts in patients with COPD. In this study we examined the effect of cigarette smoke extract (CSE) on fibroblast proliferative capacity. We found that cigarette smoke stopped proliferation of lung fibroblasts and upregulated two pathways linked to cell senescence (a biological process associated with cell longevity and an inability to replicate), p53 and p16-retinoblastoma protein pathways. We compared a single exposure of CSE to multiple exposures over an extended time course. A single exposure to CSE led to cell growth inhibition at multiple phases of the cell cycle without killing the cells. The decrease in proliferation was accompanied by increased ATM, p53, and p21 activity. However, several important senescent markers were not present in the cells at an earlier time point. When we examined multiple exposures to CSE, we found that the cells had profound growth arrest, a flat and enlarged morphology, upregulated p16, and senescence-associated β-galactosidase activity, which is consistent with a classic senescent phenotype. These observations suggest that while a single exposure to cigarette smoke inhibits normal fibroblast proliferation (required for lung repair), multiple exposures to cigarette smoke move cells into an irreversible state of senescence. This inability to repair lung injury may be an essential feature of emphysema.

Keywords: β-galactosidase; cell cycle arrest; p16; p53; senescence

Chronic obstructive pulmonary disease (COPD) is a heterogenous collection of conditions associated with an irreversible expiratory airflow limitation (1). COPD is a major public health issue and is the fourth leading cause of death in the United States (2). Cigarette smoking is a major risk factor for COPD (3, 4).

Lung fibroblasts play a crucial role in maintaining the integrity of the alveolar structures via repair of lung injury (5). Although the pathogenesis of COPD appears to be complex (6), it is clear that exposure to cigarette smoke causes lung injury (7–9). Recent studies showed that lung fibroblasts from patients with COPD have a reduced proliferation rate, a finding that suggests that cigarette smoke may both injure the lung and impair healing (10, 11). However, the mechanisms of cigarette smoke–induced fibroblast growth inhibition are unclear. We hypothesized that cigarette smoke induces fibroblast senescence, a biological state associated with cellular longevity but a reduced ability to proliferate (12).

CLINICAL RELEVANCE

This study demonstrated that cigarette smoke induces cellular senescence in lung fibroblasts with upregulation of p53 and p16 pathways. Cigarette smoke–induced senescence may cause abnormal wound healing, contributing to the pathogenesis of COPD.

Cellular senescence is defined as complete and irreversible loss of replicative capacity occurring in primary somatic cells (13). Normal human diploid fibroblasts can divide 50–70 times in tissue culture and eventually stop dividing. This type of growth arrest is referred to as replicative senescence (14). Telomeres (at the end of DNA strands) play a crucial role in replicative senescence because a loss of telomere length eventually limits cell division (15–17). Cellular senescence can be also induced by stress (stress-induced premature senescence). Exposures that are known to trigger premature senescence are hydrogen peroxide, hyperoxia, ultraviolet light, γ-irradiation (18), and oncogenic stimulation (19, 20).

The other major characteristics of a senescent cell are the following (21–23): (*1*) a distinct, flat, and enlarged cell morphology; (*2*) resistance to apoptosis; (*3*) altered production of inflammatory and growth mediators; and (*4*) an increase in senescence-associated β-galactosidase (SA β-gal) activity.

At the molecular level, cellular senescence may be induced through either or both of two pathways, the ARF-p53 pathway and p16-retinoblastoma protein (pRb) pathway (12, 24). The ARF-p53 pathway is activated by DNA damage (18), dysfunctional telomeres (25), and genotoxic stresses (26). Transcriptional activation of the INK4a/ARF locus yields p16 or ARF induction via an alternative splicing mechanism. ARF docks the mouse double minutes (MDM2) protein and quenches MDM2-dependent p53 degradation, leading to p53 accumulation. p53 accumulation also occurs downstream of ATM (27, 28). Subsequently, p53 induces proteins like p21 that cause cell cycle arrest. This cell cycle arrest cannot be reversed by growth factors, but is reversible by inactivating p53 (12).

The p16-Rb pathway is also linked to cell cycle arrest in response to DNA damage and can be activated by oncogenes or other stresses, such as suboptimal culture conditions (29). p16, an activator of pRb, docks cyclin-dependent kinases (CDK), including CDK4 and CDK6, and suppresses CDK activation through inhibition of cyclin binding, resulting in Rb activation. Activated Rb induces chromatin modifications that suppress growth-promoting transcription factors, such as E2F. Rb-induced senescence is irreversible (12).

Based on these observations, we evaluated the effects of cigarette smoke extract (CSE) on cell cycle regulation in normal lung fibroblasts. We show that a single exposure to CSE induced cell cycle arrest at multiple phases of the cell cycle. Early on, the cell cycle arrest is mediated by p53, but over time, after a

(*Received in original form May 12, 2006 and in final form July 7, 2006*)

This work was supported by a VA Merit Review grant, NIH HL-60316, NIH HL-077431 and HL079901-01A1, and RR00059 from the General Clinical Research Centers Program, NCRR, NIH, Parker B. Francis Foundation, and American Lung Association Grant RT-806-N.

Correspondence and requests for reprints should be addressed to Toru Nyunoya, M.D., Division of Pulmonary, Critical Care, and Occupational Medicine, 100 EMRB, Iowa City, IA 52242. E-mail: toru-nyunoya@uiowa.edu

Am J Respir Cell Mol Biol Vol 35. pp 681–688, 2006
Originally Published in Press as DOI: 10.1165/rcmb.2006-0169OC on July 13, 2006
Internet address: www.atsjournals.org

single exposure of CSE, the p53 levels are lost and only hypophosphorylated Rb remains. In contrast, multiple exposures to CSE results in marked upregulation of both the p53 and p16-pRb pathways. It is also associated with a flattened cellular morphology and markedly increased expression of SA β-gal activity. The cellular senescence induced by CSE is independent of telomere shortening. These data suggest that prolonged exposure to cigarette smoke induces all of the classic features of telomere-independent cellular senescence in lung fibroblasts.

MATERIALS AND METHODS

Reagents and Antibodies

Chemicals were obtained from Sigma Chemical (St. Louis, MO) and Calbiochem (La Jolla, CA). Protease inhibitors were obtained from Boehringer Mannheim (St. Louis, MO). Polyvinylidene difluoride (PVDF) membranes were obtained from Bio-Rad (Hercules, CA). ECL Plus was obtained from Amersham (Arlington Heights, IL). Antibodies were obtained from various sources: Anti-p16 and anti-p21 was from Santa Cruz Biotechnology (Santa Cruz, CA); anti-p53 and phosphorylation-specific antibodies for p53 and Rb were from Cell Signaling (Beverly, MA); anti-heat shock protein90 was from Stressgen (Victoria, BC, Canada); ATMs1981 was from Rockland (Gilbertsville, PA); anti–β-actin was from Sigma Chemical. Developing antibodies (horseradish peroxidase–conjugated anti-rabbit or anti-mouse Ig) were obtained from Santa Cruz Biotechnology. Tissue culture plates were obtained from Corning (Corning, NY).

CSE Preparation

CSE solutions were prepared using a modification of the method of Blue and Janoff (30). Through one opening of a stopcock, 10 ml of sterile Dulbecco's modified Eagle's medium (DMEM) was drawn into a 50-ml plastic syringe. Subsequently, 40 ml of cigarette smoke was drawn into the syringe and mixed with the medium by vigorous shaking. One cigarette was used for each 10 ml of medium. The generated CSE solution was filtered (0.22 μm) to remove large particles (31–34). The resulting solution was designated a 100% CSE solution. The CSE solution was used immediately after generation.

Cell Culture, Cell Count, and Cell Viability Assay

Normal human diploid lung fibroblasts, HFL-1 (American Type Culture Collection, Manassas, VA) were cultured at 37°C and in DMEM with 10% fetal bovine serum (FBS), 1% sodium pyruvate, 1% L-glutamine, and 40 μg/ml gentamicin (referred to herein as complete medium). The medium was changed every 2 d, and the cells were subcultured every 4–5 d. The fibroblasts were used between the 3rd and 8th passage. Experiments were performed in 12-well (20mm) Costar tissue culture plates at the starting cell density of $0.15–0.20 \times 10^6$/ml. The cells were incubated with or without CSE at various concentrations for various periods up to 14 d. For long-term culture experiments, in a single exposure group, fibroblasts were cultured in complete medium with CSE 5% solution for initial 48 h, and washed out with serum-free DMEM three times. The cells were then provided with complete medium every 48 h. In a multiple-exposure group, fibroblasts were cultured in complete medium with CSE 3.5% solution, and both complete medium and CSE were replaced every 48 h. In the control group, the serum media without CSE were replaced every 48 h. The cell counts were performed by an electric particle counter (Coulter Electronics, Hialeah, FL). Cell viability was analyzed by the Guava Personal Cytometer (PC) (Guava Technologies, Hayward, CA). The Guava ViaCount assay distinguishes between viable and nonviable cells based on the differential permeability of DNA-binding dyes in the ViaCount Reagent (Guava Technologies).

Senescence-Associated β-Galactosidase Activity

Senescence-associated β-galactosidase (SA β-gal) staining was performed according to a previously described method (21). Cell samples in 8-well chamber slides were fixed with 2% formaldehyde and 0.2% glutaraldehyde in PBS for 5 min at room temperature. The slides were rinsed with PBS and incubated with an SA β-gal staining solution containing 40 mM sodium citrate (pH 6.0), 150 mM NaCl, 5 mM potassium ferricyanide, 5 mM potassium ferrocyanide, 2 mM $MgCl_2$, and 1 mg/ml of 5-bromo-4-chloro-3-indoyl β-D galactoside for 4 h. For a long-term experiment, all the groups including a single exposure, multiple exposures and control were analyzed at the same time. In the control group, fibroblasts were subcultured when they became subconfluent.

Cell Cycle Synchronization with Serum Deprivation

HFL-1 cells were cultured in DMEM with 10% FBS, 1% sodium pyruvate, 1% L-glutamine and gentamicin (40 μg/ml) for 24 h. Then, the cells were washed with serum-free DMEM three times and were cultured in DMEM with 0.2% FBS, 1% sodium pyruvate, 1% L-glutamine and gentamicin (40 μg/ml) for various periods of time.

Isolation of Whole Cell Extracts

HFL-1 cells were cultured in tissue culture dishes (100 mm) with or without CSE solution of various concentrations. Whole cell protein was obtained by lysing the cells on ice for 20 min in 300 μl of lysis buffer (0.05 M Tris, pH 7.4, 0.15 M NaCl, 1% Nonidet P-40) supplemented with Complete protease inhibitors (Roche Molecular Biochemicals, Pleasanton, CA) and 1× phosphatase inhibitors (Calbiochem, La Jolla, CA). The lysates were then sonicated for 20 s, incubated on ice for 30 min, and centrifuged at $15{,}000 \times g$ for 10 min at 4°C. Protein was quantified using a protein measurement kit (Protein Assay Kit 500–0006; Bio-Rad, Hercules, CA). Cell lysates were stored at −70°C until use.

Western Blot Analysis

Western blot analysis for the presence of particular proteins or for phosphorylated forms of proteins was performed on whole cell lysates. Protein (30–60 μg) was mixed 1:1 with 2× sample buffer (20% glycerol, 4% SDS, 10% β-mercaptoethanol, 0.05% bromphenol blue, and 1.25 M Tris, pH 6.8; all from Sigma Chemical) heated to 95°C for 5 min, and fractionated on a 10% or 12.5% SDS-polyacrylamide gel run at 100 V for 90 min. Cell proteins were transferred to a PVDF membrane by semidry transfer (Bio-Rad) at 25 V for 45 min. Equal loading of the protein groups on the blots was evaluated by using anti–β-actin antibody using a staining solution designed for staining proteins on PVDF membranes. The membranes were dried completely after being soaked with 100% methanol, and then incubated with the primary antibody overnight. The blots were washed four times with Tris-buffered saline, including Tween 20, and incubated for 1 h with horseradish peroxidase–conjugated anti-rabbit or anti-mouse IgG antibody. Immunoreactive bands were developed using a chemiluminescent substrate (ECL or ECL Plus). An autoradiograph was obtained, with exposure times of 10 s to 2 min. For a long-term experiment, all the groups (including a single exposure, multiple exposures, and control) were harvested at the same time. In the control group, fibroblasts were subcultured when they became subconfluent.

Flow Cytometry

HFL-1 cells were cultured with or without CSE solution of various concentrations in regular tissue culture plates for 24 h. The cells were washed twice in PBS. They then were removed with trypsin, suspended in the original medium, and centrifuged at $300 \times g$. They then were resuspended in PBS and fixed in cold 70% ethanol overnight. After two washes in PBS, the cells were treated with 0.25 mg/ml of RNase A (Roche Molecular Biochemicals) and stained with 100 μg/ml of propidium iodide at 4°C for 30 min in the dark and analyzed for DNA content. A total of 10,000 cells that satisfied a gate on forward and side scatter to eliminate aggregates and debris were evaluated with a FACScan flow cytometer (Becton Dickinson, Mountain View, CA). Data analysis was performed with ModFit LT (Verity Software House Inc, Topsham, ME).

Statistical Analysis

The results were expressed as the mean ± SEM. The number of cells in each condition with or without the CSE solution at various time points was compared using an unpaired *t* test.

RESULTS

A Short-Term Exposure to CSE Induces Growth Inhibition, but Not All of the Classic Features of Cellular Senescence

Lung fibroblasts isolated from patients with emphysema show a decreased proliferative capacity, suggesting cellular senescence due to exposure to cigarette smoke (10, 11, 35). Senescent cells have a markedly reduced proliferative capacity, but still maintain their viability with an increase in senescence associated β-galactosidase (SA β-gal) activity (21). To evaluate this, HFL-1 cells were first cultured in the presence of various concentrations of CSE solution, and the cell density, cell viability, and SA β-gal were measured. We found that short-term exposure to CSE rapidly decreased cell proliferation in a dose-dependent manner ($P < 0.05$) (Figure 1A). We also found that the cells survived for 48 h in the presence of up to CSE 5% solution (Figure 1B). However, short-term exposure to CSE increased SA β-gal activity in only a small percentage of fibroblasts (Figure 1B). These data suggest that short-term exposure to CSE rapidly inhibits fibroblast growth, but does not induce β-gal activity for up to 48 h. The toxic activity of CSE should be labile over time as the volatile components are dissipated. Thus, we used the fresh CSE solution immediately after the generation of CSE. We also evaluated the effects of CSE filter (0.22 μm) and storage conditions on growth inhibition. Either CSE filtering or storage up to 24 h did not significantly affect CSE-induced growth inhibition (Figure 1C).

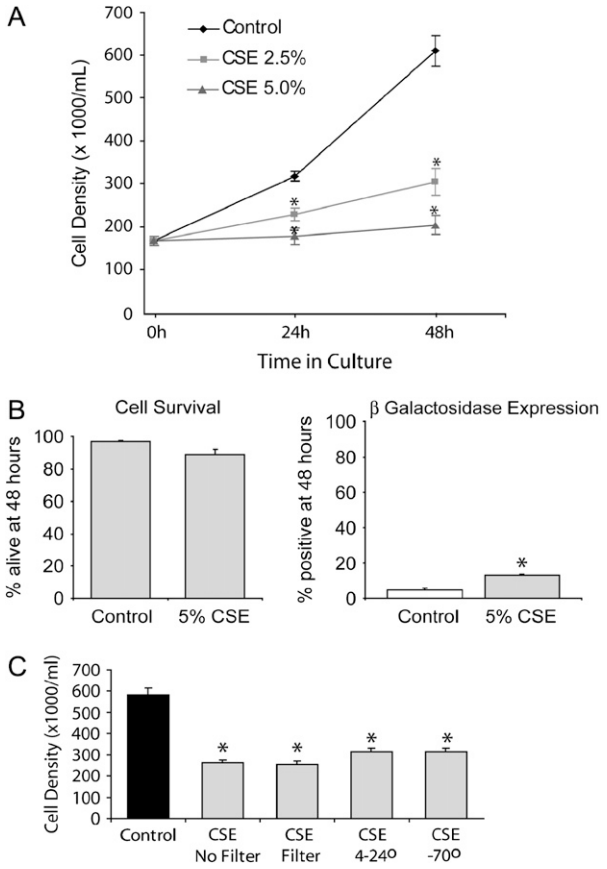

Figure 1. A short-term exposure to CSE induces growth inhibition, but not all of the classic features of cellular senescence. (*A*) HFL-1 cells were cultured in regular tissue culture plates with or without CSE 2.5 and 5% solution for 48 h. The cell counts were measured at various time points (0, 24, and 48 h). Data are expressed as mean ± SEM for three independent experiments (*$P < 0.01$). (*B*) HFL-1 cells were treated as in *A* for 48 h. The cell viability was measured by the Guava ViaCount Assay using a propidium iodide stain. Data are expressed as mean ± SEM for three independent experiments (*$P < 0.05$). SA β-gal staining was also performed at 48 h. The percentage of SA β-gal–positive cells/total cell number is shown. Data are expressed as mean ± SEM for three independent experiments (*$P < 0.05$). (*C*) HFL-1 cells were cultured at the starting cell density of 0.15×10^6/ml in regular tissue culture plates with or without CSE 5% solution. CSE was prepared with or without filtering (0.22 μm) for the immediate use, and filtered CSE solution was kept at 4°C or −70°C for 24 h before use. The cell counts were measured at 48 h. Data are expressed as mean ± SEM for three independent experiments (*$P < 0.05$).

A Single Exposure to CSE Induces Cell Cycle Arrest at Multiple Phases of the Cell Cycle

The mechanisms by which CSE affects the fibroblast cell cycle are not well elucidated. To evaluate this, we studied fibroblasts at different cell cycle phases with propidium iodide staining for DNA content and evaluated cell cycle by flow cytometry. We found that fibroblasts synchronized by serum deprivation (accumulation of cells in the G1 phase) did not respond to serum restitution if they were exposed to CSE 5% solution (Figure 2A). In contrast, CSE treatment of asynchronous fibroblasts resulted in accumulation of the cells in the S and G2 phases of the cell cycle (Figure 2B). The asynchronous fibroblasts did not increase in the cell number after CSE exposure (Figure 1A), even with an increase in the cells in S and G2 phases. This indicates that exposure to CSE induces G1 arrest in presynchronized fibroblasts and S and G2 arrest in asynchronous fibroblasts. In all of these conditions, there was no apparent increase in subdiploid (apoptotic) cells after exposure to CSE 5% solution up to 48 h (data not shown). To confirm CSE-induced cell cycle arrest in both presynchronized and asynchronous fibroblasts, we also performed a cell proliferation assay using Carboxyfluorescein diacetate, succinimidyl ester (CFSE). A short-term exposure to CSE inhibited fluorescent dilution of CFSE-labeled cells at 48 hours (data not shown). Moreover, we evaluated the activity of a mitosis marker, phosphorylation of histone H3. Exposure to CSE significantly decreased phosphorylation of histone H3 consistent with cell cycle arrest (Figure 2C). These observations suggest that CSE is capable of blocking multiple phases of the cell cycle.

A Single Exposure to CSE Causes an Early Activation of the ATM-p53-p21-pRb Pathway

Kim and coworkers recently reported that exposure to CSE can cause DNA damage in lung fibroblasts (34). It is known that some oxidative stresses such as hyperoxia can damage DNA and induce cell cycle arrest via ATM-p53-p21 pathway (36, 37). The downstream target, a retinoblastoma protein (pRb) can be activated (hypophosphorylated) through induction of cyclin-dependent kinase inhibitors (CDKIs), such as p21, a transcriptional target of p53, or p16 in response to DNA damage (38, 39). For this reason, we analyzed the effect of CSE on activity of ATM, p53, and pRb and accumulation of p53, p21, and p16. Fibroblasts were cultured in the presence of CSE 5% solution for 24 h. Western blot analysis was performed for phosphorylation (active state) of ATM (serine 1981) and p53 (serine 15), hyperphosphorylation (inactive state) of pRb and the amount of p53, p21, and p16. As shown in Figure 3A, exposure to CSE induced activation of ATM, p53, and pRb, a marked increase in p53 and p21, and a mild increase in p16 accumulation. These results indicate that CSE-induced cell cycle arrest is linked at early time points to an activation of ATM-p53-p21-Rb pathway and, to a lesser extent, p16-Rb pathway. To examine whether these changes were prolonged, we examined cells with a single CSE

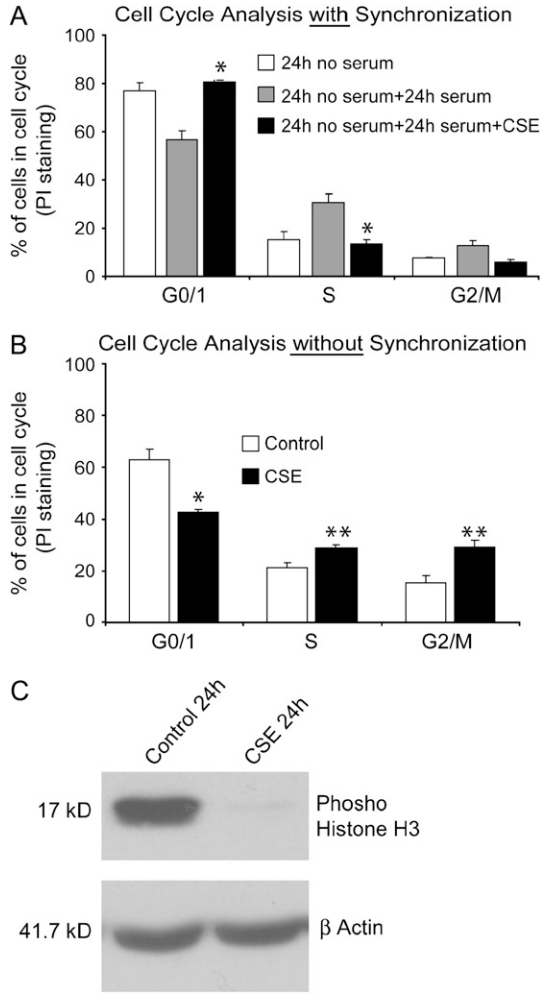

Figure 2. A single exposure to CSE induces cell cycle arrest at multiple phases of the cell cycle. (*A*) Cell cycle synchronization was induced with serum deprivation. Then, HFL-1 cells were cultured with or without CSE 5% solution in the presence of serum in regular tissue culture plates for 24 h. The harvested cells were stained with propidium iodide and were evaluated with a FACScan flow cytometer. The percentage of cells at each cell cycle phase/total cells was shown. Data are expressed as mean ± SEM for three independent experiments (*$P < 0.05$). (*B*) HFL-1 cells were treated as in *A*, except that they were not synchronized by prior exposure to serum deprivation. The percentage of cells at each cell cycle phase/total cells is shown. Data are expressed as mean ± SEM for three independent experiments (*$P < 0.01$; **$P < 0.05$). (C) HFL-1 cells were cultured with or without CSE 5% solution for 24 h. Western blot analysis was performed for phosphorylation of Histone 3 (Ser 10) at 24 h. Equal loading was determined by stripping the blot and re-probing with antibodies to β-actin. Western blotting data are representative of three experiments.

exposure up to 14 d. We found that a delayed response to CSE was accompanied by significant p16 upregulation and persistent pRb activation, while the increases in p53 disappeared by 14 d after exposure (Figure 3B). Notably, the delayed response to a single exposure to CSE was associated with a significant increase in SA β-gal activity. As a composite, these data suggest that a single exposure to CSE causes sequential activation from p53 to p16-pRb pathway with a moderate increase in SA β-gal activity for a prolonged period.

Multiple Exposures to CSE Induce Cellular Senescence

Patients with COPD are repetitively exposed to cigarette smoke. Thus, multiple exposures to CSE should be more relevant, physiologically. We hypothesized that multiple exposures to CSE induce cellular senescence. To evaluate this, fibroblasts were cultured with a single exposure to CSE 5% solution for 48 h followed by washout, and incubation with a CSE-free complete medium or multiple exposures to CSE 3.5% solution for up to 2 wk (the lower concentration of CSE was chosen for multiple exposures in order to maintain fibroblast viability). The cell density was measured on Days 0, 2, 4, 7, and 14. In a group that had undergone single CSE exposure, the fibroblasts were growing slowly; however, the growth rate was still slower compared to the control group for up to 2 wk. In contrast, multiple exposures to CSE almost completely inhibited cell growth (Figure 4A). The CSE-exposed cells were still viable (data not shown). Next we measured SA β-gal activity in the cells that underwent multiple CSE exposures. As shown on Figure 4B, multiple exposures to CSE ultimately increased SA β-gal activity and induced a flat and enlarged cell morphology. These data suggest that multiple exposures more reliably induce senescence in a majority of cells compared with a single exposure.

CSE-Induced Cellular Senescence Is Linked to Activation of Both p16-pRb and p53 Pathways

Cellular senescence may be induced through either or both of two pathways: (*1*) the p53 pathway, and/or (*2*) the pRb pathway (12). It is known that stress-induced premature senescence is associated with activation of both pathways (24). Thus, we hypothesized that profound CSE-induced cellular senescence should be accompanied by activation of both p53 and p16-pRb pathways. To evaluate this, fibroblasts were cultured with multiple exposures to CSE 3.5% solution for 2 wk. Western blot analysis was performed for p53 and p16 accumulation and pRb activity in the CSE-exposed fibroblasts on Days 7 and 14. As shown in Figure 5, multiple exposures to CSE markedly increased p53 and p16 accumulation and activated pRb. Chronic exposure to cigarette smoke has been linked to the development of p53 mutations (40). We evaluated the downstream effect of p53 with p21 accumulation up to 2 wk. Exposure to CSE increased p21 up to 2 wk (data not shown). This suggests that the p53 function is intact for up to 2-wk of exposure to CSE. These data suggest that multiple exposures to CSE reliably trigger all of the classic features of stress-induced cellular senescence.

It is known that replicative senescence occurs through telomere shortening (41). However, it has been reported that stress-induced premature senescence can be independent of telomere shortening (42). To determine if CSE causes telomere shortening, fibroblasts were cultured with continuous exposure to CSE 3.5% solution for up to 2 wk. The length of telomeres was determined as a relative telomere to single copy gene (36B4) (T/S) ratio measured by RT-PCR. As expected, prolonged exposure to CSE did not shorten telomere for up to 2 wk (data not shown). This suggests that cigarette smoke–induced cellular senescence may occur through telomere-independent signals.

DISCUSSION

We show that, in normal human lung fibroblasts, prolonged exposure (multiple exposures) to CSE induces cellular senescence with a characteristic flattened cell morphology and a marked increase in SA β-gal activity. This senescence phenotype is accompanied by activation of both the p53 and p16 pathways. Both of these pathways likely contribute to the cell cycle arrest that is typical of cellular senescence. By contrast, a single exposure to CSE induces only some of the features of cellular senescence.

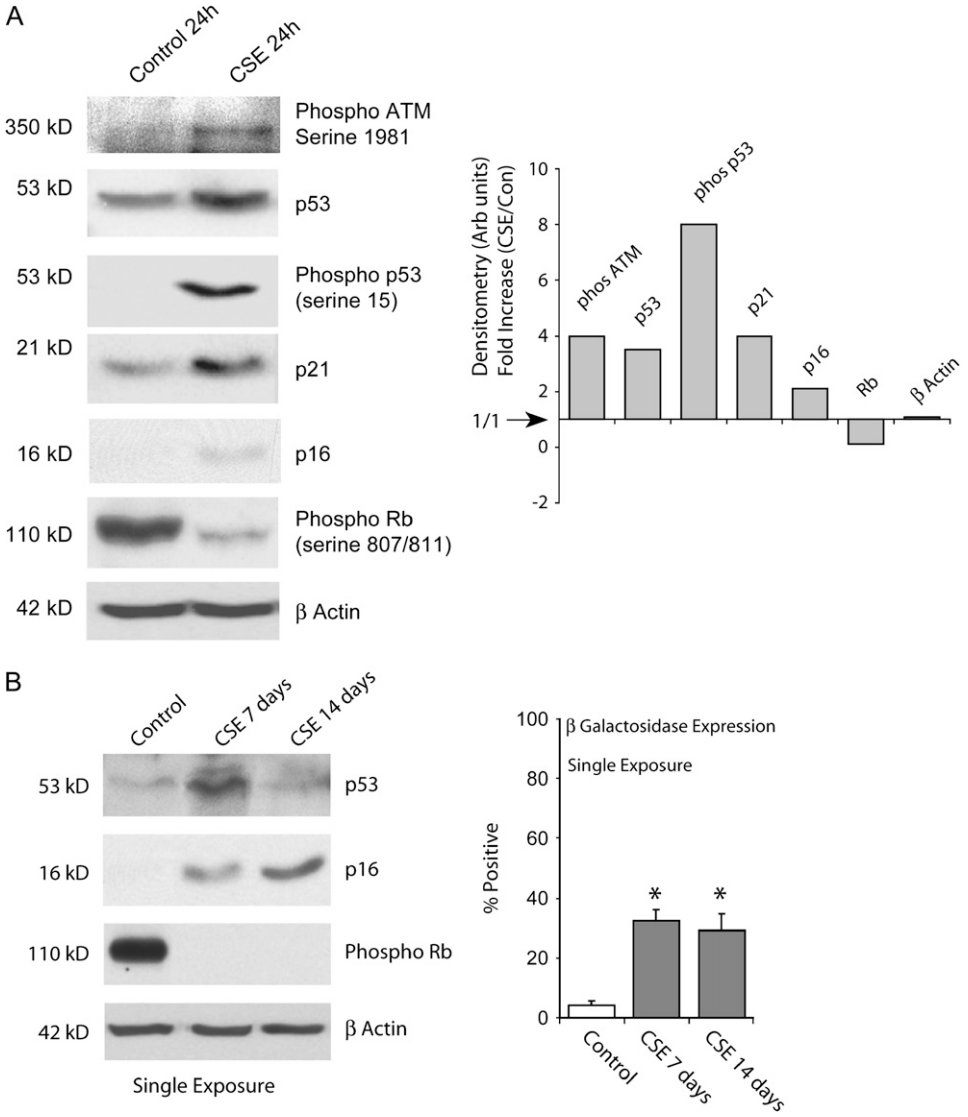

Figure 3. A single exposure to CSE causes an early activation of the ATM-p53-p21-pRb pathway. (*A*) HFL-1 cells were cultured with or without CSE 5% solution for 24 h. Western blot analysis was performed for phosphorylation of ATM (serine 1981), p53 (serine 15), and pRb (serine 807/811) and the amount of p53, p21, and p16 at 24 h. Equal loading was determined by stripping the blot and reprobing with antibodies to β-actin. Western blotting data are representative of three experiments. (*B*) HFL-1 cells were cultured with or without CSE 5% solution for 48 h, and were washed out, then were cultured with a serum media for up to 2 wk. Western blot analysis was performed for phosphorylation of pRb (inactive state) and the amount of p53 and p16. Equal loading was determined by stripping the blot and reprobing with antibodies to β-actin. Western blotting data are representative of three experiments. HFL-1 cells were treated as in *B.* SA β-gal staining was performed at 7 d and at 14 d. The percentage of SA β-gal–positive cells/total cell number is shown. Data are expressed as mean ± SEM for three independent experiments (*$P < 0.01$).

These data suggest that a prolonged and repeated use of cigarette smoke induces cellular senescence, potentially contributing to the pathogenesis of COPD. One important result of a lack of proliferation of lung fibroblasts is an inability to repair the injury induced by CSE.

Several studies have evaluated the effects of cigarette smoke on cell proliferation in lung fibroblasts. An *in vitro* study has shown that exposure to CSE significantly inhibits fibroblast proliferation (43). Other studies have also demonstrated that fibroblasts isolated from patients with emphysema have a decreased capacity for proliferation (10, 11, 35). None of these studies provided a mechanism for the decreased fibroblast proliferation associated with cigarette smoke exposure. Our data provide a biological mechanism for this effect of CSE on lung fibroblasts. We found that exposure to CSE induces cell cycle arrest at multiple phases of the cell cycle (G0/1, S, and G2) in fibroblasts. This appears to be mediated by activation of both the p53 and p16 pathways, which have profound effects on the cell cycle. In individuals who smoke, susceptibility of lung fibroblasts to cigarette smoke–induced cellular senescence may be altered by the genetic phenotype of the patient, explaining why some, but not all, individuals who smoke develop emphysema.

It is known that exposure to CSE induces DNA damage (34). Cells respond to DNA damage by activating checkpoint pathways such as the p53 and p16 pathways to inhibit cell cycle progression (12, 44). Cellular senescence can be induced by either or both of these pathways. Although there is some cross-talk between the two pathways, p53-dependent senescence is primarily induced by oxidative stresses, DNA damage, and telomere dysfunction. Recent *in vitro* studies showed that exposure to some oxidant stresses induces p53-dependent senescence in cultured fibroblasts (45) and endothelial progenitor cells (46). The p16 pathway is often associated with senescence due to oncogenes and various stresses, including suboptimal culture conditions (19, 47). It is known, however, that DNA damage can also activate the p16 pathway after transient p53 activation to induce premature senescence (39). Moreover, p16 can be upregulated in replicative senescence. In some cells, p16 gene expression and protein accumulation are progressively increased with cell divisions (48, 49). A recent animal study also supported this, because the p16 gene expression was markedly increased in almost all organs with aging (50). In our study, we found that exposure to CSE increases the p16 protein in a time-dependent manner (at least up to 7 d), even with a single exposure. Multiple exposures to CSE also ultimately activate the p53 pathway, but

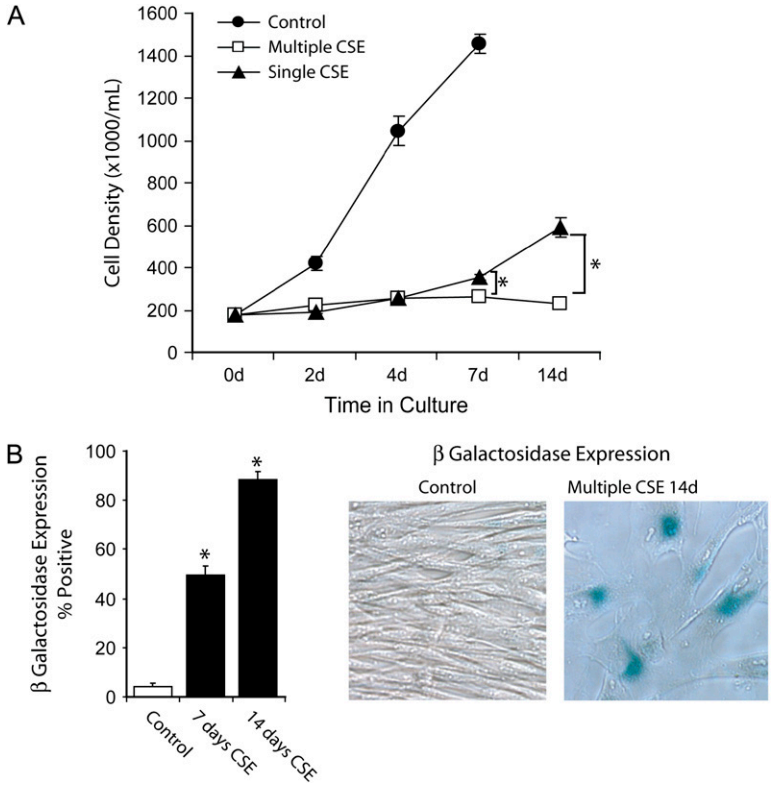

Figure 4. Multiple exposures to CSE induce cellular senescence. (*A*) HFL-1 cells were cultured on regular tissue culture plates with multiple exposures to CSE 3.5% solution or a single exposure to CSE 5% solution (for 48 h followed by no exposure to CSE for an additional 12 d) or without CSE for up to 14 d. The cell counts were measured at various time points (Days 0, 2, 4, 7 and 14). Data are expressed as mean ± SEM for three independent experiments (*$P < 0.01$). (*B*) HFL-1 cells were treated as in *A.* SA β-gal staining was performed for the control and multiple CSE-exposed cells on Days 7 and 14. The percentage of SA β-gal–positive cells/total cell number was shown. Data are expressed as mean ± SEM for three independent experiments (*$P < 0.01$). The *digital photographs* were obtained on Day 14, and represent one of three identical experiments.

with a single exposure p53 accumulation is gradually lost over the following 2 wk. This coordinated activity of p16 and p53 correlates well with the growth rate in fibroblast cell density data (Figure 4A), and both pathways likely contribute to a fibroblast senescent phenotype, including cell cycle arrest, an increase in SA β-gal activity, and a flat and enlarged morphology (Figure 6).

SA β-gal is a hydrolase located at the lysosomes (51, 52). Lysosomal β-gal splits β-linked terminal galactosyl residues from some substrates, such as gangliosides. However, the mechanisms and roles of an increase in SA β-gal activity in senescent cells remain to be elucidated (53). Some lack of specificity to senescent cells limits the utility of SA β-gal, because some conditions such as confluence (54) and serum deprivation (55) may increase the activity. However, SA β-gal is still widely used for a biomarker for cellular senescence (24). Both *in vitro* and *in vivo* studies also support that SA β-gal activity correlates with p16 expression (21, 50). In our study, SA β-gal activity appears to be upregulated with both p16 and p53 accumulation.

Telomere shortening is responsible for replicative senescence. Telomerase overexpression to extend short telomeres can prolong life-span in mortal somatic cells (17). In contrast, stress-induced premature senescence may or may not be accompanied by telomere shortening. Mild oxidative stresses, such as mild hyperoxia, can rapidly shorten the telomere length in the stress-induced senescent cells (56, 57). An *in vitro* study demonstrated that the other oxidant stresses such as hydrogen peroxide, irradiation, and ultraviolet light did not erode the telomeres in cultured human fibroblasts (42). Consistent with this study finding, we found that exposure to CSE did not shorten the telomere length (data not shown). Whether or not stress-induced premature senescence is accompanied by telomere attrition may be dependent on the intensity of the oxidative stress. A mild oxidative stress

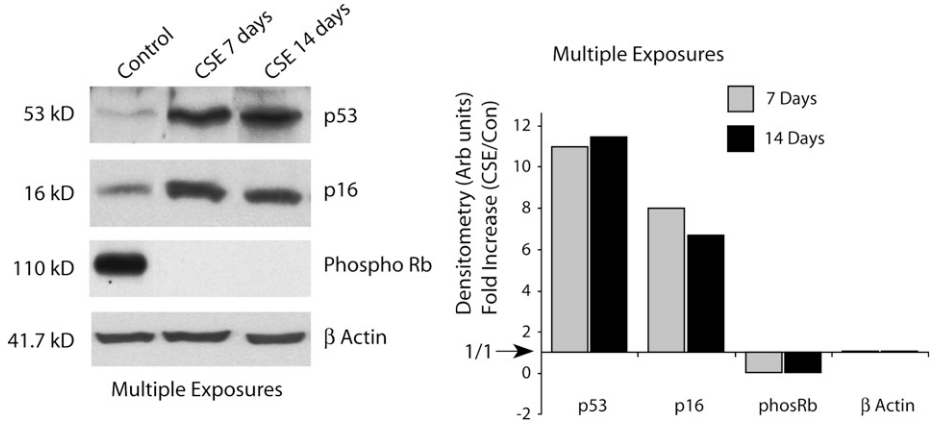

Figure 5. CSE-induced cellular senescence is linked to activation of both the p16 and p53 pathways. HFL-1 cells were cultured on regular tissue culture plates with multiple exposures to CSE 3.5% solution for up to 14 d. Western blot analysis was performed for accumulation of p53 and p16 and phosphorylation of pRb. Equal loading was determined by stripping the blot and reprobing with antibodies to β-actin. Western blotting data are representative of three experiments.

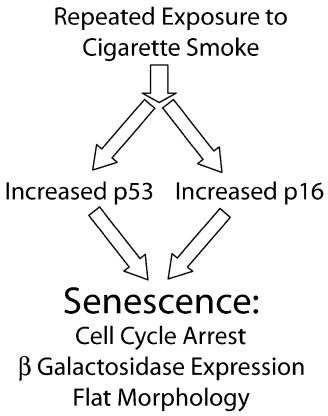

Figure 6. A proposed pathway for CSE-induced cellular senescence. Repeated exposure to CSE activates both the p53 and p16 pathways. Both pathways likely contribute to a senescent phenotype, including cell cycle arrest, an increase in SA β-gal activity, and a flat and enlarged cellular morphology.

that allows the cells to proliferate may rapidly shorten the telomere length. In contrast, a strong oxidative stress may not erode the telomere because the cells cannot proliferate.

Effects of cigarette smoke on cellular senescence do not appear to be specific to the cell type. Tsuji and colleagues showed that exposure to cigarette smoke induces cellular senescence in alveolar epithelial cells of both *in vitro* and animal models. Interestingly, they showed that cigarette smoke induces epithelial senescence before emphysema develops in a mouse model (33). These data suggest that cellular senescence may contribute to COPD pathogenesis. However, it is still unclear which cell type is more sensitive to cigarette smoke–induced cellular senescence, and which cell type of senescence is more significant for COPD pathogenesis.

In conclusion, this study demonstrates that, in human lung fibroblasts, prolonged (repeated) exposure to CSE induces a senescent phenotype with cell cycle arrest, a flattened cell morphology, and a marked increase in SA β-gal activity. Some of these changes occurred with a single exposure to CSE; however, full senescence required multiple exposures. This CSE induced premature senescence was accompanied by activation of both p53 and p16 pathways and was not associated with telomere shortening. These data imply that a prolonged (or repeated) *in vivo* exposure to cigarette smoke may trigger cellular senescence in lung fibroblasts. Cigarette smoke–induced cellular senescence may play a role in abnormal wound healing, preventing repair of lung injury. This may contribute to the pathogenesis of COPD.

Conflict of Interest Statement: None of the authors has a financial relationship with a commercial entity that has an interest in the subject of this manuscript.

References

1. Pauwels RA, Buist AS, Calverley PM, Jenkins CR, Hurd SS. Global strategy for the diagnosis, management, and prevention of chronic obstructive pulmonary disease. NHLBI/WHO Global Initiative for Chronic Obstructive Lung Disease (GOLD) Workshop summary. *Am J Respir Crit Care Med* 2001;163:1256–1276.
2. Murphy SL. Deaths: final data for 1998. *Natl Vital Stat Rep* 2000;48:1–105.
3. Mannino DM, Homa DM, Akinbami LJ, Ford ES, Redd SC. Chronic obstructive pulmonary disease surveillance--United States, 1971–2000. *MMWR Surveill Summ* 2002;51:1–16.
4. Fishman AP. One hundred years of COPD. *Am J Respir Crit Care Med* 2005;171:941–948.
5. Absher M. Fibroblasts. In: Massaro D, editor. Lung biology in health and disease. New York: Marcel Dekker Inc.; 1995. pp. 401–439.
6. Shapiro SD, Ingenito EP. The pathogenesis of chronic obstructive pulmonary disease: advances in the past 100 years. *Am J Respir Cell Mol Biol* 2005;32:367–372.
7. Ma B, Kang MJ, Lee CG, Chapoval S, Liu W, Chen Q, Coyle AJ, Lora JM, Picarella D, Homer RJ, *et al.* Role of CCR5 in IFN-gamma-induced and cigarette smoke-induced emphysema. *J Clin Invest* 2005;115:3460–3472.
8. Hogg JC, Chu F, Utokaparch S, Woods R, Elliott WM, Buzatu L, Cherniack RM, Rogers RM, Sciurba FC, Coxson HO, *et al.* The nature of small-airway obstruction in chronic obstructive pulmonary disease. *N Engl J Med* 2004;350:2645–2653.
9. Spira A, Beane J, Pinto-Plata V, Kadar A, Liu G, Shah V, Celli B, Brody JS. Gene expression profiling of human lung tissue from smokers with severe emphysema. *Am J Respir Cell Mol Biol* 2004;31:601–610.
10. Noordhoek JA, Postma DS, Chong LL, Vos JT, Kauffman HF, Timens W, van Straaten JF. Different proliferative capacity of lung fibroblasts obtained from control subjects and patients with emphysema. *Exp Lung Res* 2003;29:291–302.
11. Holz O, Zuhlke I, Jaksztat E, Muller KC, Welker L, Nakashima M, Diemel KD, Branscheid D, Magnussen H, Jorres RA. Lung fibroblasts from patients with emphysema show a reduced proliferation rate in culture. *Eur Respir J* 2004;24:575–579.
12. Campisi J. Senescent cells, tumor suppression, and organismal aging: good citizens, bad neighbors. *Cell* 2005;120:513–522.
13. Hayflick L, Moorhead PS. The serial cultivation of human diploid cell strains. *Exp Cell Res* 1961;25:585–621.
14. Serrano M, Blasco MA. Putting the stress on senescence. *Curr Opin Cell Biol* 2001;13:748–753.
15. Olovnikov AM. A theory of marginotomy: the incomplete copying of template margin in enzymic synthesis of polynucleotides and biological significance of the phenomenon. *J Theor Biol* 1973;41:181–190.
16. Harley CB, Futcher AB, Greider CW. Telomeres shorten during ageing of human fibroblasts. *Nature* 1990;345:458–460.
17. Bodnar AG, Ouellette M, Frolkis M, Holt SE, Chiu CP, Morin GB, Harley CB, Shay JW, Lichtsteiner S, Wright WE. Extension of life-span by introduction of telomerase into normal human cells. *Science* 1998;279:349–352.
18. Di Leonardo A, Linke SP, Clarkin K, Wahl GM. DNA damage triggers a prolonged p53-dependent G1 arrest and long-term induction of Cip1 in normal human fibroblasts. *Genes Dev* 1994;8:2540–2551.
19. Serrano M, Lin AW, McCurrach ME, Beach D, Lowe SW. Oncogenic ras provokes premature cell senescence associated with accumulation of p53 and p16INK4a. *Cell* 1997;88:593–602.
20. Zhu J, Woods D, McMahon M, Bishop JM. Senescence of human fibroblasts induced by oncogenic Raf. *Genes Dev* 1998;12:2997–3007.
21. Dimri GP, Lee X, Basile G, Acosta M, Scott G, Roskelley C, Medrano EE, Linskens M, Rubelj I, Pereira-Smith O, *et al.* A biomarker that identifies senescent human cells in culture and in aging skin in vivo. *Proc Natl Acad Sci USA* 1995;92:9363–9367.
22. Marcotte R, Lacelle C, Wang E. Senescent fibroblasts resist apoptosis by downregulating caspase-3. *Mech Ageing Dev* 2004;125:777–783.
23. Wang E. Senescent human fibroblasts resist programmed cell death, and failure to suppress bcl2 is involved. *Cancer Res* 1995;55:2284–2292.
24. Satyanarayana A, Rudolph KL. p16 and ARF: activation of teenage proteins in old age. *J Clin Invest* 2004;114:1237–1240.
25. Herbig U, Jobling WA, Chen BP, Chen DJ, Sedivy JM. Telomere shortening triggers senescence of human cells through a pathway involving ATM, p53, and p21(CIP1), but not p16(INK4a). *Mol Cell* 2004;14:501–513.
26. Taylor LM, James A, Schuller CE, Brce J, Lock RB, Mackenzie KL. Inactivation of p16INK4a, with retention of pRB and p53/p21cip1 function, in human MRC5 fibroblasts that overcome a telomere-independent crisis during immortalization. *J Biol Chem* 2004;279:43634–43645.
27. Zhang X, Li J, Sejas DP, Pang Q. The ATM/p53/p21 pathway influences cell fate decision between apoptosis and senescence in reoxygenated hematopoietic progenitor cells. *J Biol Chem* 2005;280:19635–19640.
28. Moiseeva O, Mallette FA, Mukhopadhyay UK, Moores A, Ferbeyre G. DNA damage signaling and p53-dependent senescence after prolonged beta-interferon stimulation. *Mol Biol Cell* 2006;17:1583–1592.
29. Sherr CJ, McCormick F. The RB and p53 pathways in cancer. *Cancer Cell* 2002;2:103–112.
30. Blue ML, Janoff A. Possible mechanisms of emphysema in cigarette smokers. Release of elastase from human polymorphonuclear leukocytes by cigarette smoke condensate in vitro. *Am Rev Respir Dis* 1978;117:317–325.
31. Carnevali S, Petruzzelli S, Longoni B, Vanacore R, Barale R, Cipollini M, Scatena F, Paggiaro P, Celi A, Giuntini C. Cigarette smoke extract induces oxidative stress and apoptosis in human lung fibroblasts. *Am J Physiol Lung Cell Mol Physiol* 2003;284:L955–L963.
32. Panayiotidis MI, Stabler SP, Allen RH, Ahmad A, White CW. Cigarette smoke extract increases S-adenosylmethionine and cystathionine in

human lung epithelial-like (A549) cells. *Chem Biol Interact* 2004;147: 87–97.
33. Tsuji T, Aoshiba K, Nagai A. Cigarette smoke induces senescence in alveolar epithelial cells. *Am J Respir Cell Mol Biol* 2004;31:643–649.
34. Kim H, Liu X, Kobayashi T, Conner H, Kohyama T, Wen FQ, Fang Q, Abe S, Bitterman P, Rennard SI. Reversible cigarette smoke extract-induced DNA damage in human lung fibroblasts. *Am J Respir Cell Mol Biol* 2004;31:483–490.
35. Nobukuni S, Watanabe K, Inoue J, Wen FQ, Tamaru N, Yoshida M. Cigarette smoke inhibits the growth of lung fibroblasts from patients with pulmonary emphysema. *Respirology* 2002;7:217–223.
36. Helt CE, Rancourt RC, Staversky RJ, O'Reilly MA. p53-dependent induction of p21(Cip1/WAF1/Sdi1) protects against oxygen-induced toxicity. *Toxicol Sci* 2001;63:214–222.
37. Helt CE, Cliby WA, Keng PC, Bambara RA, O'Reilly MA. Ataxia telangiectasia mutated (ATM) and ATM and Rad3-related protein exhibit selective target specificities in response to different forms of DNA damage. *J Biol Chem* 2005;280:1186–1192.
38. O'Reilly MA. Redox activation of p21Cip1/WAF1/Sdi1: a multifunctional regulator of cell survival and death. *Antioxid Redox Signal* 2005;7:108–118.
39. Robles SJ, Adami GR. Agents that cause DNA double strand breaks lead to p16INK4a enrichment and the premature senescence of normal fibroblasts. *Oncogene* 1998;16:1113–1123.
40. Toyooka S, Tsuda T, Gazdar AF. The TP53 gene, tobacco exposure, and lung cancer. *Hum Mutat* 2003;21:229–239.
41. Campisi J. The biology of replicative senescence. *Eur J Cancer* 1997;33: 703–709.
42. Gorbunova V, Seluanov A, Pereira-Smith OM. Expression of human telomerase (hTERT) does not prevent stress-induced senescence in normal human fibroblasts but protects the cells from stress-induced apoptosis and necrosis. *J Biol Chem* 2002;277:38540–38549.
43. Nakamura Y, Romberger DJ, Tate L, Ertl RF, Kawamoto M, Adachi Y, Mio T, Sisson JH, Spurzem JR, Rennard SI. Cigarette smoke inhibits lung fibroblast proliferation and chemotaxis. *Am J Respir Crit Care Med* 1995;151:1497–1503.
44. Bartek J, Lukas C, Lukas J. Checking on DNA damage in S phase. *Nat Rev Mol Cell Biol* 2004;5:792–804.
45. Catalano A, Rodilossi S, Caprari P, Coppola V, Procopio A. 5-Lipoxygenase regulates senescence-like growth arrest by promoting ROS-dependent p53 activation. *EMBO J* 2005;24:170–179.
46. Rosso A, Balsamo A, Gambino R, Dentelli P, Falcioni R, Cassader M, Pegoraro L, Pagano G, Brizzi MF. p53 Mediates the accelerated onset of senescence of endothelial progenitor cells in diabetes. *J Biol Chem* 2006;281:4339–4347.
47. Lin AW, Barradas M, Stone JC, van Aelst L, Serrano M, Lowe SW. Premature senescence involving p53 and p16 is activated in response to constitutive MEK/MAPK mitogenic signaling. *Genes Dev* 1998;12: 3008–3019.
48. Hara E, Smith R, Parry D, Tahara H, Stone S, Peters G. Regulation of p16CDKN2 expression and its implications for cell immortalization and senescence. *Mol Cell Biol* 1996;16:859–867.
49. Alcorta DA, Xiong Y, Phelps D, Hannon G, Beach D, Barrett JC. Involvement of the cyclin-dependent kinase inhibitor p16 (INK4a) in replicative senescence of normal human fibroblasts. *Proc Natl Acad Sci USA* 1996;93:13742–13747.
50. Krishnamurthy J, Torrice C, Ramsey MR, Kovalev GI, Al-Regaiey K, Su L, Sharpless NE. Ink4a/Arf expression is a biomarker of aging. *J Clin Invest* 2004;114:1299–1307.
51. Kurz DJ, Decary S, Hong Y, Erusalimsky JD. Senescence-associated (beta)-galactosidase reflects an increase in lysosomal mass during replicative ageing of human endothelial cells. *J Cell Sci* 2000;113:3613–3622.
52. Lee BY, Han JA, Im JS, Morrone A, Johung K, Goodwin EC, Kleijer WJ, Dimaio D, Hwang ES. Senescence-associated beta-galactosidase is lysosomal beta-galactosidase. *Aging Cell* 2006;5:187–195.
53. Cristofalo VJ. SA beta Gal staining: biomarker or delusion. *Exp Gerontol* 2005;40:836–838.
54. Severino J, Allen RG, Balin S, Balin A, Cristofalo VJ. Is beta-galactosidase staining a marker of senescence in vitro and in vivo? *Exp Cell Res* 2000;257:162–171.
55. Yegorov YE, Akimov SS, Hass R, Zelenin AV, Prudovsky IA. Endogenous beta-galactosidase activity in continuously nonproliferating cells. *Exp Cell Res* 1998;243:207–211.
56. von Zglinicki T, Saretzki G, Docke W, Lotze C. Mild hyperoxia shortens telomeres and inhibits proliferation of fibroblasts: a model for senescence? *Exp Cell Res* 1995;220:186–193.
57. Vaziri H, West MD, Allsopp RC, Davison TS, Wu YS, Arrowsmith CH, Poirier GG, Benchimol S. ATM-dependent telomere loss in aging human diploid fibroblasts and DNA damage lead to the post-translational activation of p53 protein involving poly(ADP-ribose) polymerase. *EMBO J* 1997;16:6018–6033.